15th International Congress on Artificial Materials for Novel Wave Phenomena – Metamaterials 2021
New York, USA, Aug. 2nd –7th, 2021

Artificial intelligence enabled classification of subwavelength objects from far-field scattering

S. Kurdiumov [1], J.Y. Ou [1], N. Papasimakis [1] and N.I. Zheludev [1,2]

[1] Optoelectronics Research Centre & Centre for Photonic Metamaterials, University of Southampton, SO17 1BJ, United Kingdom
[2] Centre for Disruptive Photonic Technologies, The Photonics Institute, School of Physical and Mathematical Sciences, Nanyang Technological University, 637371 Singapore.
sk1u19@soton.ac.uk; niz@orc.soton.ac.uk

***Abstract* – We demonstrate shape classification of deeply subwavelength objects with accuracy exceeding 90% by machine learning analysis of far-field scattering patterns.**

Reconstruction of an object based on its far-field scattering pattern is an ill-posed problem placing fundamental limits in imaging and microscopy. Recently, artificial intelligence approaches have been put forward as means to surpass such limitations, promising imaging at resolution orders of magnitude beyond the ~λ/2 diffraction limit [1]. Here, we show that a neural network processing of far-field scattering patterns allows shape classification of deeply subwavelength objects (<λ/2) with accuracy better than 90%.

We demonstrate shape classification by numerical experiments, in which a plane wave is scattered through an aperture of unknown size and shape in an opaque screen (see Fig. 1a). The size of the aperture ranges between λ/10 and λ/2, while its shape is selected from 11 different geometrical shapes: circle, equilateral triangle, square, hexagon, ellipsis, zigzag, line, rectangle, ring, star and Y-shape. The aperture is positioned at the center of the opaque screen and is illuminated with a linearly polarised monochromatic plane wave. A dataset of 50,000 two-dimensional diffraction patterns is then recorded at a distance of 2λ with a field of view of 15λx15λ. Classification of geometry shapes is performed by a fully-connected neural network, which contains 8 dense layers. 80% of data (40,000 samples) was used for training, 10% (5,000 samples) - for validation and the remaining 10% (5,000) - for testing. Typical diffraction patterns for different objects of size λ/3 are depicted in Fig. 1b. Although the diffraction patterns for all three objects appear similar, a closer look reveals differences in the scattered field distribution (see Fig. 1b right column).

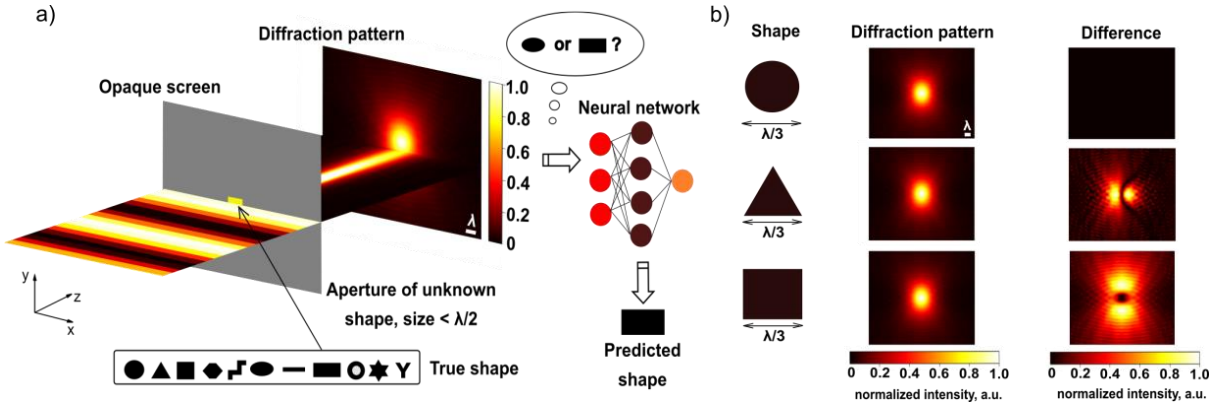

Fig. 1. (a) Schematic illustration of the subwavelength object classification process. An aperture of randomly selected geometrical shape in an opaque screen is illuminated with an x-polarized plane wave. The diffraction pattern is collected at the distance z=2λ away from the object and then fed into a neural network, which retrieves the shape of the object. (b) Diffraction patterns from three different objects (circle, triangle and square of the same size λ/3 placed at the centre of the field of view (FOV)) and their differences from the reference (circle of size λ/3). All diffraction patterns and differences are normalized to their maximum value. The FOV is 15λx15λ.

Results of the shape classification are presented in the form of a confusion matrix. The horizontal axis represents the predicted shapes, and the vertical axis represents the true labels. For example, the first row (hexagon) indicates that 82% of the images labelled as hexagon are correctly classified, while 18% were wrongly classified as stars. All elements in each row are normalised to the number of true shapes corresponding to this row. Overall, the accuracy of the classification process, i.e. the number of correctly classified objects over the total number of objects in the dataset, is 95%. Here we see that the most challenging task for the network is to distinguish hexagons from stars, which we attribute to the hexagonal symmetry of both shapes and the finite spatial resolution in our numerical calculations (λ/40). On the other hand, lines, zigzags and rings are the most distinguishable shapes. To further characterize the performance of our approach, we employ precision and recall as metrics. Precision for a given class (shape) is defined as the ratio of the number of objects correctly classified in the given class (true positives) over the total number of objects, correctly and incorrectly classified in the given class (true positives and false positives). Similarly, recall for a given class is defined as the ratio of thea number of objects correctly classified in the given class (true positives) over the total number of objects belonging to the given class (true positives and false negatives). To understand the limits of the technique we studied how the performance of the method depends on the number of shapes and the dataset size. The results of this study are depicted in Fig. 2b. The overall accuracy decreases with the growing number of geometry shapes and increases with the dataset size (number of samples for training, validation and test, added together). Thus, to achieve overall accuracy over 90% for two shapes a dataset of 1,000 samples is needed, while for 5 and 10 shapes the required dataset size grows to 5,000 and 50,000, respectively.

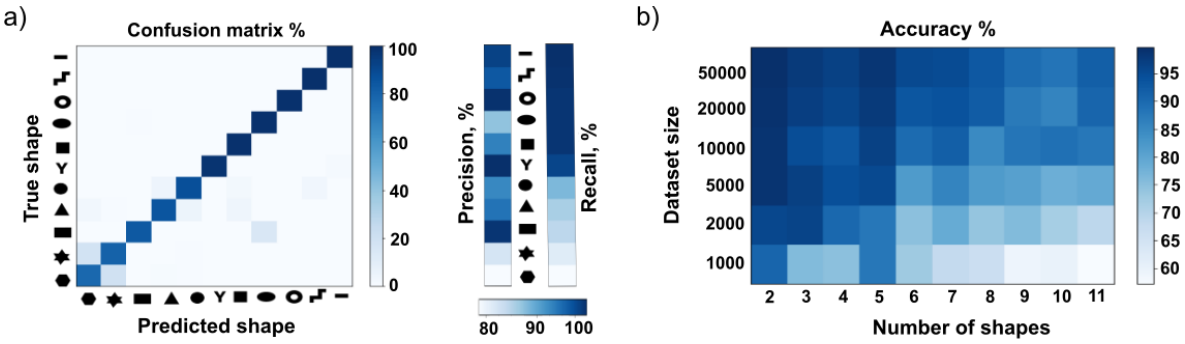

Fig. 2. (a) Performance of the shape classification process quantified by accuracy (left) and precision and recall (right). The classification was performed for the dataset of 11 different shapes containing 5,000 samples (test dataset). The number of samples of each shape is different within 10%. (b) Dependence of accuracy on the dataset size and the number of shapes. Shapes were arranged in the datasets in the following order: circle and square were in the initial dataset of 2 shapes, then, subsequently, triangle, rectangle, ellipsis, hexagon, zigzag, line, ring, star and Y-shape were added.

In conclusion, we demonstrate the classification of deeply subwavelength objects in terms of their geometrical shape with accuracy better than 90%. Our approach is based on processing far-field diffraction patterns by artificial intelligence. The proposed technique may find applications in biomedical sciences and nanotechnology.

REFERENCES

[1] T. Pu, J. Y. Ou, V. Savinov, G. Yuan, N. Papasimakis and N. Zheludev, "Unlabelled Far-Field Deeply Subwavelength Topological Microscopy (DSTM) Adv. Sci. 8(1), 2002886 (2020)